

THREE-DIMENSIONAL THEORY FOR A SMITH-PURCELL FREE-ELECTRON LASER WITH GRATING SIDEWALLS

H. L. Andrews*, C. A. Brau, J. D. Jarvis

Department of Physics and Astronomy, Vanderbilt University, Nashville, Tennessee, 37235, USA

Abstract

We present an analytic theory for the operation of a Smith-Purcell free-electron laser with side walls that includes the effects of transverse diffraction in the optical beam. We allow the width of the electron beam and the width of the grating to vary independently, and require the walls be high compared with the wavelength of the evanescent wave. The results show that the side walls change the empty-grating dispersion relation in important ways. When the separation of the walls is not too large, it is sufficient to consider only the lowest-order transverse mode of the grating. For this case we obtain excellent agreement with numerical simulations and experimental data.

INTRODUCTION

The wide range of potential applications for terahertz (THz) radiation in fields such as biology, chemistry and materials science is currently driving interest in the development of intense, compact, tunable THz sources [1, 2]. Electron-beam-based slow wave structures are very promising sources of THz radiation. Slow-wave structures support subluminal electromagnetic modes, which may interact resonantly with an electron beam passing in close proximity. This resonant interaction causes bunching in the electron beam and amplitude growth of the optical field. Superradiant Smith-Purcell radiation may be extracted from an open grating structure[3], a configuration known as a Smith-Purcell free-electron laser (SPFEL). The SPFEL may be operated as an amplifier (convective instability), or as an oscillator (absolute instability), depending on the sign of the laser waves group velocity. The 2-D theory of such a device has been examined in detail for the exponential gain/growth regime [4, 5, 6, 9] and is closely supported by particle-in cell (PIC) numerical simulations [6, 7, 8]. In addition, we have considered analytically the effects of transverse diffraction in a 3-D theory without side walls [10].

In this work, we include the effects of transverse diffraction in the optical beam of an SPFEL including confinement of the beam by side walls. The results show that the presence of side walls changes in the dispersion relation significantly. Excellent agreement is obtained when the results are compared to numerical simulations using a PIC code [11] and experimental data [13].

* heather.l.andrews@vanderbilt.edu

DISPERSION

In a SPFEL, resonant energy exchange between the electron beam and bound surface modes gives rise to spatial modulations in the beam density. These density modulations lead to superradiant enhancement of the emitted SP-radiation, and subsequent modification of its angular distribution [3]. The intensity scale height of the evanescent wave is $\Delta x = \beta\gamma\lambda/4\pi \approx 40 \mu\text{m}$ for the parameters of Table 1, where $\beta = 0.34$ is the normalized electron velocity, $\gamma = 1/\sqrt{1-\beta^2}$, and $\lambda \approx 10^{-3}$ m is the free-space wavelength.

Table 1: Grating and beam parameters used in calculations.

| | |
|-------------------------|-------------------|
| Grating period | 157 μm |
| Grating width | 610 μm |
| Slot depth | 226 μm |
| Slot width | 61 μm |
| Grating length | 7.85 mm |
| Beam energy | 30 keV |
| Beam width/height | 44 μm |
| Beam current | 10 mA |
| Height of beam centroid | 35 μm |

A schematic of the device geometry with all pertinent dimensions is given in Figures 1 and 2. Because the fields vanish exponentially above the scale height, we allow the electron beam to extend to infinity in x .

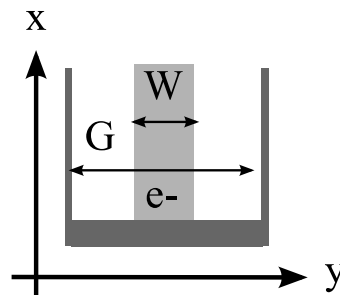


Figure 1: View looking down the grating in the three-dimensional model. The electron beam has a width W and is allowed to extend to infinity in x . The side wall spacing, or grating width, is G and the walls extend to infinity in x .

In the following analysis we calculate the fields subject to the Maxwell equations and boundary conditions and solve for the dispersion relation. We then intro-

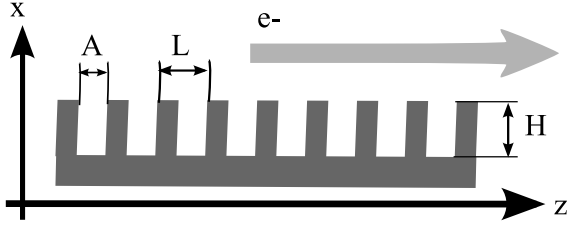


Figure 2: View of the grating from the side (walls omitted). The grating period is L , slot depth H and slot width A . The electron beam travels in the $+z$ direction.

duce the electron beam as a perturbation and calculate the resulting wavenumber and frequency shifts for solutions to the dispersion relation. To first order, the electron beam will only couple with transverse-magnetic modes, so transverse-electric modes are not considered.

Experience has shown [6] that the fields in the grooves are nearly uniform in the z direction, so we express the fields inside the grooves as Fourier series of the form

$$E_z^{(g)} = \sum_{r=0}^{\infty} E_r^{(g)} \sin[\kappa_r(x+H)] \cos\left[(2r+1)\frac{\pi y}{G}\right] e^{-i\omega t}$$

$$H_y^{(g)} = \sum_{r=0}^{\infty} H_r^{(g)} \cos[\kappa_r(x+H)] \cos\left[(2r+1)\frac{\pi y}{G}\right] e^{-i\omega t}$$

where ω is the frequency. Each term in the fields must satisfy the wave equation, which is given in the grooves by

$$\kappa_r^2 + (2r+1)^2 \frac{\pi^2}{G^2} - \frac{\omega^2}{c^2} = 0$$

Above the grating we expand the fields in Floquet series of the form

$$E_z^{(e)} = \sum_{r=0}^{\infty} \sum_{p=-\infty}^{\infty} E_p^{(e)} e^{-\alpha_{rp}x} \cos\left[(2r+1)\frac{\pi y}{G}\right] e^{ipKz} e^{i(kz-\omega t)}$$

$$H_y^{(e)} = \sum_{r=0}^{\infty} \sum_{p=-\infty}^{\infty} H_p^{(e)} e^{-\alpha_{rp}x} \cos\left[(2r+1)\frac{\pi y}{G}\right] e^{ipKz} e^{i(kz-\omega t)}$$

where k is the longitudinal wavenumber, and $K = 2\pi/L$ is the grating wave number. The electron beam is treated as an isotropic plasma dielectric in its rest frame, the primed coordinates, having an index of refraction given by [12]

$$n'(\omega') = 1 + \chi_e'(\omega') = 1 - \frac{\omega_e'^2}{\omega'^2}$$

where $\chi_e' = -\frac{\omega_e'^2}{\omega'^2}$ is the frequency-dependent susceptibility and ω_e' is the plasma frequency. Since $(k+pK) - \frac{\omega_p^2}{c^2}$, $E_p^{(e)}$ and the transverse dimensions, x and y , are Lorentz invariant, the wave equation above the grating becomes

$$\alpha_{rp}^2 - (2r+1)^2 \frac{\pi^2}{G^2} - (k+pK)^2 + \frac{\omega^2}{c^2} - \frac{\omega_e'^2}{c^2} = 0. \quad (1)$$

Using the parameters in Table 1, we find the plasma frequency to be $\approx 10^{10}$ Hz, and the operating frequency

FEL Theory

$\approx 10^{12}$ Hz, allowing us to ignore the last term in equation (1) and find that α_{rp} is constant across the width of the grating.

When we use the Maxwell-Ampere law and Gauss law to relate the electric and magnetic field components and require that the tangential electric and magnetic fields be continuous at the surface of the grating, we arrive at the dispersion relation

$$D_s E_s^{(g)} = \sum_{r=0}^{\infty} R_{sr} E_r^{(g)} \quad (2)$$

where

$$D_s = 1 + \frac{L \sin(\kappa_s H)}{A \cos(\kappa_s H)} \sum_{p=-\infty}^{\infty} \frac{\omega^2 K_p^* K_p}{\omega^2 - (k+pK)^2 c^2} \frac{\alpha_{sp}}{\kappa_s}$$

$$R_{sr} = \frac{L \omega^2 K_0^* K_0}{A \omega^2 - k^2 c^2} \frac{\omega_e^2}{\gamma^3 (\omega - \beta c k)^2} \frac{\alpha_{r0}}{\kappa_s} J_{rs} \frac{\sin(\kappa_r H)}{\cos(\kappa_r H)}$$

are the dispersion function for the r^{th} transverse component and the coupling matrix respectively.

In the absence of the electron beam, the dispersion relation $\omega_r(k)$ for mode r is found from $D_r(\omega, k) = 0$. This is shown in Figure 3 for parameters of Table 1. Also shown is the beam line $\omega = \beta c k$. The synchronous points shown there are the points where the modes have a phase velocity equal to the velocity of the electrons in the beam. The group velocity for each mode is the slope of the dispersion curve, $\beta_r c = d\omega_r/dk$. We note that for the parameters in Table 1, the group velocity is negative for all r . Also shown in Figure 3 is the dispersion curve predicted by the 2-D theory [6]. The group velocity in this theory is positive.

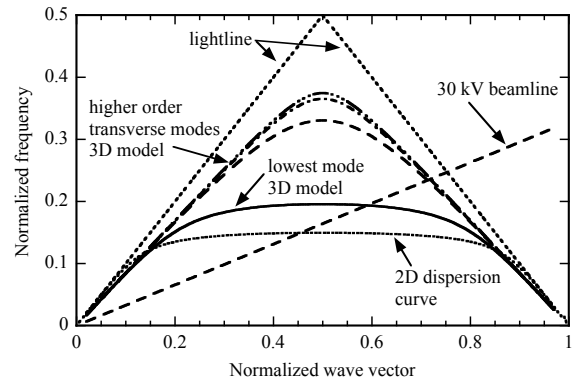


Figure 3: The dispersion relations for the 2D theory [6] and 3D theory with walls for the first 4 transverse modes, plotted with the beam line for 30 kV and light lines. The 2D theory predicts a $\sim 900 \mu\text{m}$ forward wave, while the 3D theory predicts a $\sim 790 \mu\text{m}$ backward wave. The higher transverse modes are well separated from the $r = 0$ mode.

When the electron beam is present we define $\epsilon_r = D_r E_r^{(g)}$ and $T_{sr} = R_{sr}/D_r$ so that the dispersion relation

becomes an eigenvalue equation

$$\epsilon_s = \sum_{r=0}^{\infty} T_{sr} \epsilon_r = \lambda \epsilon_s. \quad (3)$$

where $\lambda = 1$.

This equation must be solved numerically. To provide a starting value for the solution algorithm, we need an approximate solution of (3), or equivalently (2). We begin by observing that when gain is maximized, the walls of the grating are as narrow as possible. When the grating is narrow, the modes are widely spaced, as shown in Figure 3 and the solution is dominated by the lowest transverse mode $r = 0$. Also when the electron beam fills most of the grating, the overlap integrals J_{rs} are small for $r \neq s$, so the coupling matrix R_{sr} is nearly diagonal. Therefore, on the right-hand side of (3) we ignore all modes except $r = s$. For the lowest-order mode we find $D_0(\omega, k) = R_{00}(\omega, k)$.

We expect that the gain will be maximal near the synchronous point (ω_0, k_0) where $D_0(\omega_0, k_0) = 0$ and $\omega_0 = \beta c k_0$. Near this point we expand

$$D_0(\omega, k) \approx D_\omega \delta\omega + D_k \delta k \quad (4)$$

where $\delta\omega = \omega - \omega_0$, $\delta k = k - k_0$, $D_\omega(\omega_0, k_0) = \frac{\partial D_0}{\partial \omega}(\omega_0, k_0)$ and $D_k(\omega_0, k_0) = \frac{\partial D_0}{\partial k}(\omega_0, k_0)$. But along the dispersion curve, D_ω and D_k are related by

$$\frac{dD_0}{dk} = 0 = \frac{\partial D_0}{\partial k} + \frac{\partial D_0}{\partial \omega} \frac{\partial \omega}{\partial k} = D_k + \beta_0 c D_\omega$$

This allows us to rewrite the dispersion function as $D_0(\omega, k) \cong D_\omega(\delta\omega - \beta_0 c \delta k)$. Including these approximations, the dispersion relation becomes

$$(\delta\omega - \beta_0 c \delta k)^2 (\delta\omega - \beta_0 c \delta k) = \frac{\omega_e^2 Q_{00}(\omega_0, k_0)}{\gamma^3 D_\omega(\omega_0, k_0)}$$

where $Q_{sr}(\omega, k) = R_{sr}(\omega - \beta c k)$. This has the same form as the 2-D theory, so we can take advantage of the analysis used for that case [6].

AMPLIFIER

When the device operates as a steady-state amplifier, $\delta\omega = 0$ and β_0 is positive. The dispersion relation becomes

$$\delta k^3 = -\frac{\omega_e^2}{\beta^2 \beta_0 \gamma^3 c^3} \frac{Q_{00}(\omega_0, k_0)}{D_\omega(\omega_0, k_0)}$$

This has three roots. Calculations show that D_ω and Q_{00} are both negative, irrespective of the operating voltage, so the roots are

$$\delta k_n = \left| \frac{\omega_e^2}{\beta^2 \beta_0 \gamma^3 c^3} \frac{Q_{00}(\omega_0, k_0)}{D_\omega(\omega_0, k_0)} \right|^{\frac{1}{3}} e^{i \frac{2\pi}{3} n} \quad (5)$$

for $n = 0, 1, 2$. The gain is the imaginary part of the root with the most negative imaginary part, so we see that the gain is

$$\mu = \frac{\sqrt{3}}{2} \left| \frac{\omega_e^2}{\beta^2 \beta_0 \gamma^3 c^3} \frac{Q_{00}(\omega_0, k_0)}{D_\omega(\omega_0, k_0)} \right|^{\frac{1}{3}}$$

Starting with the three approximate roots given by (5), we can solve the exact dispersion relation (3) to find the gain. The results are shown in Figure 4, where we see that for the parameters in Table 1 the approximate calculation of the gain is quite close to the exact solution. The mode is dominated by the lowest-order component, $r = 0$, and the Taylor expansion (5) is justified.

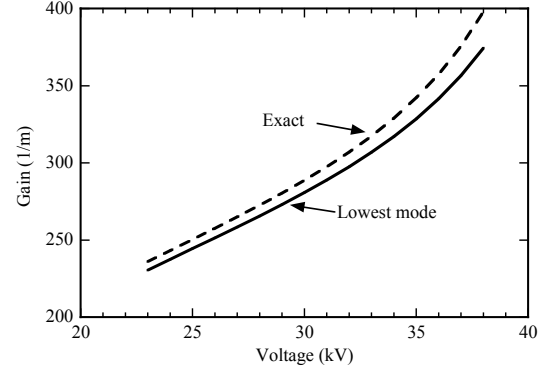


Figure 4: Gain as a function of electron beam energy for the lowest mode and the exact solution considering mode mixing. Gain is dominated by the contribution from the lowest mode.

OSCILLATOR

When the synchronous point lies to the right of the Bragg point, the group velocity is negative and the device operates on an absolute instability [5]. Above a certain current, called the start current, the device oscillates spontaneously. In this case, both the frequency shift and the wave number shift are nonvanishing. For a solution to exist three boundary conditions must be satisfied in conjunction with the dispersion relation. The electron beam must be free of density and velocity modulations at the upstream end of the grating, and the input optical field at the downstream end must vanish [6]. In general, the fields corresponding to the three roots of the homogeneous dispersion relation have different transverse profiles, and the boundary conditions cannot be satisfied for all y . In cases of practical interest, the solution is dominated by the lowest-order component $r = 0$, as discussed above. The three roots have the same profile and can interfere to satisfy the boundary conditions for all y . We further assume that the Taylor-series expansion used above to compute the approximate solution of the dispersion relation remains valid. The analysis is then the same as that used previously for the 2-D theory [6]. The three waves corresponding to the three roots of the dispersion relation become locked together to form the mode of the oscillator. All the waves have the same complex frequency shift $\delta\omega$, but different wave number shifts, so they interfere constructively and destructively to satisfy the boundary conditions.

As a test of these predictions, we can compare our results to the simulations by Dazhi Li [11]. The parameters

are summarized in Table 1. In the simulations the electron beam fills only the region between $h_b = 13 \mu\text{m}$ and $h_t = 57 \mu\text{m}$, whereas in the theory the beam extends to infinity. To correct for this we reduce the current density by the filling factor $F = \exp(-h_b\alpha_{0,-1}) - \exp(-h_t\alpha_{0,-1})$ where $1/\alpha_{0,-1}$ is the scale height of the evanescent wave [6]. As shown in Figure 5, the agreement with simulations is remarkably good.

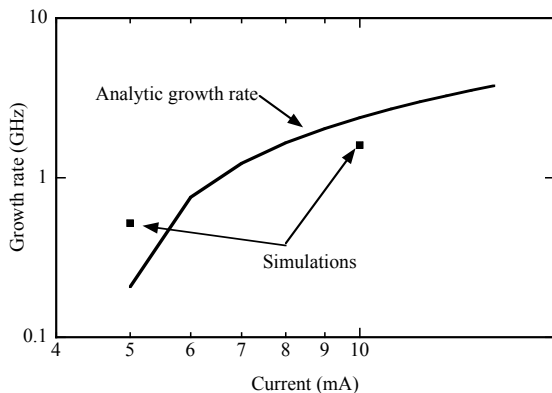


Figure 5: Growth rate as a function of electron beam current compared with PIC code simulations [11]. The results show remarkable agreement.

In Figure 6 we compare the operating wavelength predicted by this theory with that observed in recent experiments [13]. The agreement is quite good.

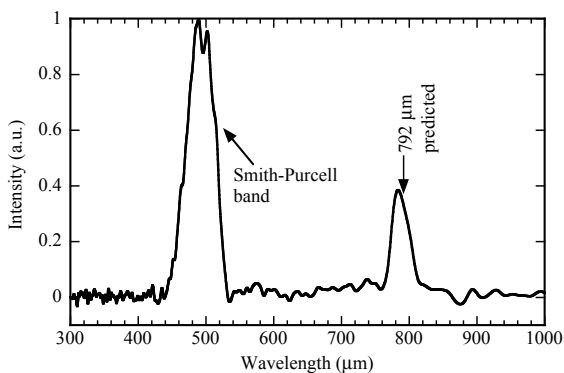


Figure 6: Spectrum from recent experiments at Vermont Photonics [13] compared with predicted operating wavelength. The agreement is very good.

CONCLUSIONS

We present a theory of operation for an SPFEL with grating side walls. We find that gain and growth rate are increased over the 2-D and 3-D theory without walls. We also find remarkable agreement when comparing the predicted growth rate with PIC code simulations, and the predicted wavelengths with experimental observations.

ACKNOWLEDGEMENTS

The authors gratefully acknowledge helpful discussions with Dazhi Li. This work was supported by the Medical Free Electron Laser Program and the Department of Defense under grant number F49620-01-1-0429.

REFERENCES

- [1] P. H. Siegel, IEEE Trans. Microwave Theory and Techniques 50, 910 (2002).
- [2] S. P. Micken and X.-C. Zhang, Int. J. High Speed Electron. 13, 601 (2003).
- [3] H. L. Andrews, C. H. Boulware, C. A. Brau and J. D. Jarvis, Phys. Rev. ST Accel. Beams 8, 110702 (2005).
- [4] H. L. Andrews and C. A. Brau, Phys. Rev. ST Accel. Beams 7, 070701 (2004).
- [5] H. L. Andrews, C. H. Boulware, C. A. Brau and J. D. Jarvis, Phys. Rev. ST Accel. Beams 8, 050703 (2005).
- [6] H. L. Andrews, C. H. Boulware, C. A. Brau, J. T. Donohue, J. Gardelle and J. D. Jarvis, New J. Phys. 8, 298 (2006).
- [7] D. Li, Z. Yang, K. Imasaki and Gun-Sik Park, Phys. Rev. ST Accel. Beams 9, 040701 (2006).
- [8] J. T. Donohue and J. Gardelle, Phys. Rev. ST Accel. Beams 8, 060702 (2005).
- [9] V. Kumar and K-J Kim, Phys. Rev. E 73, 026501 (2006).
- [10] J. D. Jarvis and H. L. Andrews, "Three-Dimensional theory of the Smith-Purcell free-electron laser", 29th International Free-Electron Laser Conference, Novosibirsk, Russia, August 2007.
- [11] Dazhi Li, private communication.
- [12] C. A. Brau, *Modern Problems in Classical Electrodynamics*(Oxford, New York, 2004), p. 345.
- [13] H. L. Andrews, C. A. Brau, J. D. Jarvis, C. F. Guertin, A. O'Donnell, B. Durant, T. H. Lowell and M. R. Mross, "Experimental Observation of the Evanescent Wave in a Smith-Purcell Free-Electron Laser", 30th International Free-Electron Laser Conference, Gyeongju, Korea, August 2008.